

## Supporting Information

### **Trimetallic nanocomposites developed for efficient *in vivo* bimodal imaging via fluorescence and magnetic resonance**

*Veronika Svačinová*<sup>1</sup>, *Aminadav Halili*<sup>2</sup>, *Radek Ostruszka*<sup>1</sup>, *Tomáš Pluháček*<sup>3</sup>, *Klára Jiráková*<sup>2,4</sup>, *Daniel Jiráček*<sup>2,5</sup>, *Karolína Šišková*<sup>1,\*</sup>

<sup>1</sup>Department of Experimental Physics, Faculty of Science, Palacký University Olomouc, tř. 17. Listopadu 12, 77900 Olomouc, Czech Republic

<sup>2</sup>Institute for Clinical and Experimental Medicine, Videnska 9, 140 21 Prague, Czech Republic

<sup>3</sup>Department of Analytical Chemistry, Faculty of Science, Palacký University Olomouc, tř. 17. Listopadu 12, 77900 Olomouc, Czech Republic

<sup>4</sup>Department of Histology and Embryology, The Third Faculty of Medicine, Charles University, Ruská 87, 100 00 Prague, Czech Republic

<sup>5</sup>Faculty of Health Studies, Technical University of Liberec, Studentska 1402/2, 46117 Liberec, Czech Republic

\*Corresponding author (K.Š.) email and phone no.: karolina.siskova@upol.cz; Tel.: +420-585-634-175

#### ***Table of contents:***

1. ICP-MS (pages 2-3)
2. Mössbauer spectroscopy of LGSN-SPION (page 4)
3. DLS measurements of LGSN-SPION (page 5)
4. Excitation-emission luminescence 3D map (page 6)
5. Quantum yield determined for LGSN-SPION via SPION-free sample (page 7)
6. Photo-stability of LGSN-SPION in media (page 8-9)
7. Cell viability evaluated for LGSN-SPION (page 10)
8. *In vitro* optical imaging using LGSN-SPION (page 11)
9. *In vivo* optical imaging using LGSN-SPION (page 12)
10. Results of relaxometry measurements of LGSN-SPION (page 13-14)
11. T<sub>1</sub>-weighted MR images of phantoms (page 15)

## 1. ICP-MS

**Table SI-1:** Theoretical and experimental (determined by ICP-MS) values of metal concentrations (expressed in mM) in LGSN-SPION nanocomposite after the dialysis.

Protein	Au		Ag		Fe	
c(th) [mM]	c(th) [mM]	c(exp) [mM]	c(th) [mM]	c(exp) [mM]	c(th) [mM]	c(exp) [mM]
0.30	6.06	5.14	1.52	1.51	6.06	5.66
		5.15		1.50		5.65
		5.07		1.50		5.74
<b>Average value</b>	n.a.	5.12 ± 0.04	n.a.	1.50 ± 0.01	n.a.	5.68 ± 0.05

### ICP-MS method

The ICP-MS method utilized a microwave-assisted digestion step to decompose organic matrix. The power-controlled digestion program is presented in Table SI-2. However, the optimized ICP-MS method parameters are summarized in Table SI-3.

**Table SI-2:** Power-controlled digestion program

Step	Power (W)	Time (min)
1	250	2
2	0	2
3	400	5
4	0	2
5	500	2
6	0	2
7	600	7

ventilation: 5 minutes

**Table SI-3:** Optimized ICP-MS parameters

RF power (W)	1550
Plasma gas flow rate (L/min)	15.0
Auxiliary gas flow rate (L/min)	0.9
Nebuliser gas flow rate (L/min)	1.05
He gas flow rate (mL/min)	4.3
Dwell time (ms)	100
Monitored isotopes	<sup>45</sup> Sc (IS), <sup>56</sup> Fe, <sup>107</sup> Ag, <sup>115</sup> In (IS), <sup>197</sup> Au, <sup>209</sup> Bi (IS)

IS – internal standard

### ICP-MS method validation

The modified method was revalidated in terms of linearity, limit of detection, limit of quantification, trueness, precision (T&P tested at the concentration level of 500 µg/L). The validation strategy and data for Au and Fe are summarized in the previously published work (*Ostruszka et al. 2023*), whereas the results for Ag are summarized in Table SI-3. Calculated recoveries for Ag, Fe, and Au in repeatedly measured QC samples (n=4) were 94 %, 97%, 95%.

**Table SI-4:** Validation results for silver

Parameter	Ag
Calibration range ( $\mu\text{g/L}$ )	10 – 2 000
Correlation coefficient	1.0000
LOD ( $\mu\text{g/L}$ )	1
LOQ ( $\mu\text{g/L}$ )	3
Trueness (%)	96.8
Precision (%)	0.9

**Reference:** R. Ostruszka, D. Půlpánová, T. Pluháček, O. Tomanec, P. Novák, D. Jiráček, K. Šišková, Facile One-Pot Green Synthesis of Magneto-Luminescent Bimetallic Nanocomposites with Potential as Dual Imaging Agent, *Nanomaterials*. 13 (2023) 1027. <https://doi.org/10.3390/nano13061027>.

## 2. Mössbauer spectroscopy of LGSN-SPION

Experimental description: A home-made Mössbauer spectrometer was used to determine the oxidation and spin state of iron atoms within LGSN-SPION samples. A representative as-prepared and centrifuged LGSN-SPION sample was measured with an OLTWINS Mössbauer spectrometer in the transmission mode (made by *Procházka and co-workers*), using a constant acceleration rate and  $^{57}\text{Co}$  (Rh) source. The isomer shift values were related to the 28  $\mu\text{m}$   $\alpha\text{-Fe}$  foil (Ritverc) measured at room temperature. The acquired Mössbauer spectrum was processed using MossWinn 4.0 software (*Klencsár et al, 1996*).

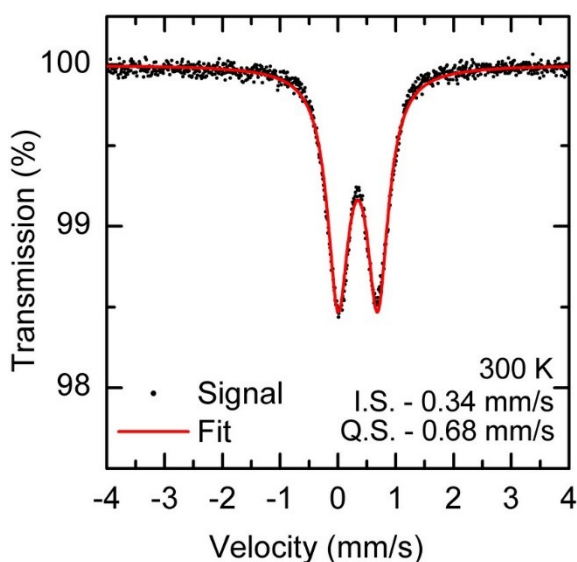


**Figure SI-1:** Mössbauer spectrum of a representative LGSN-SPION sample.

Isomer shift and quadrupole splitting values (within the experimental error) well correspond to iron (III) oxide nanoparticles evidenced also in (*R. Ostruszka et al. 2023*).

### References:

- Klencsár, Z.; Kuzmann, E.; Vértes, A. User-Friendly Software for Mössbauer Spectrum Analysis. *J. Radioanal. Nucl. Chem. Artic.* **1996**, 210, 105–118.
- Ostruszka R., Půlpánová D., Pluháček T., Tomanec O., Novák P., Jiráček D., Šišková K., Facile One-Pot Green Synthesis of Magneto-Luminescent Bimetallic Nanocomposites with Potential as Dual Imaging Agent, *Nanomaterials*. 13 (2023) 1027. <https://doi.org/10.3390/nano13061027>
- Procházka, V.; Novák, P.; Stejskal, A. Department of Experimental Physics. Mössbauer Spectrometers OLTWINS. Available online: <http://oltwins.upol.cz/> (accessed on 6 February 2024).

### 3. DLS measurements of LGSN-SPION

**Table SI-5:** Average values determined for LGSN-SPION nanocomposite when measured by dynamic light scattering (DLS): Z-average, polydispersity index (PDI), hydrodynamic diameter (based on intensity changes measurements), and zeta potential.

Z-Average [nm]	PDI	Size (intensity) [nm]	Zeta potential [mV]
$214.5 \pm 3.4$	$0.31 \pm 0.03$	$301.9 \pm 8.4$	$-43.8 \pm 2.0$

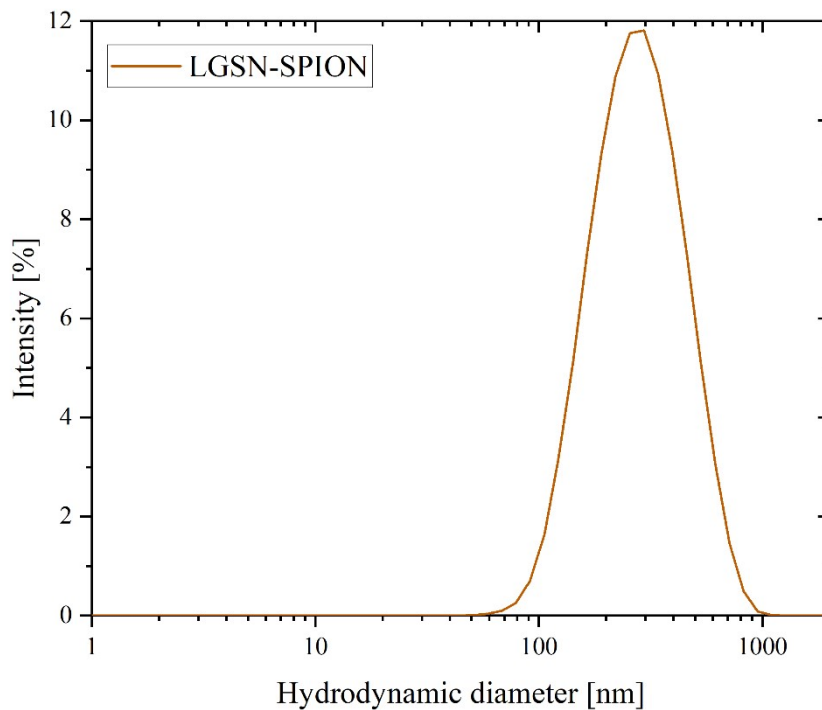


**Figure SI-2:** Particle size distribution of LGSN-SPION nanocomposite based on changes of scattered light intensity.

#### 4. Excitation-emission luminescence 3D map

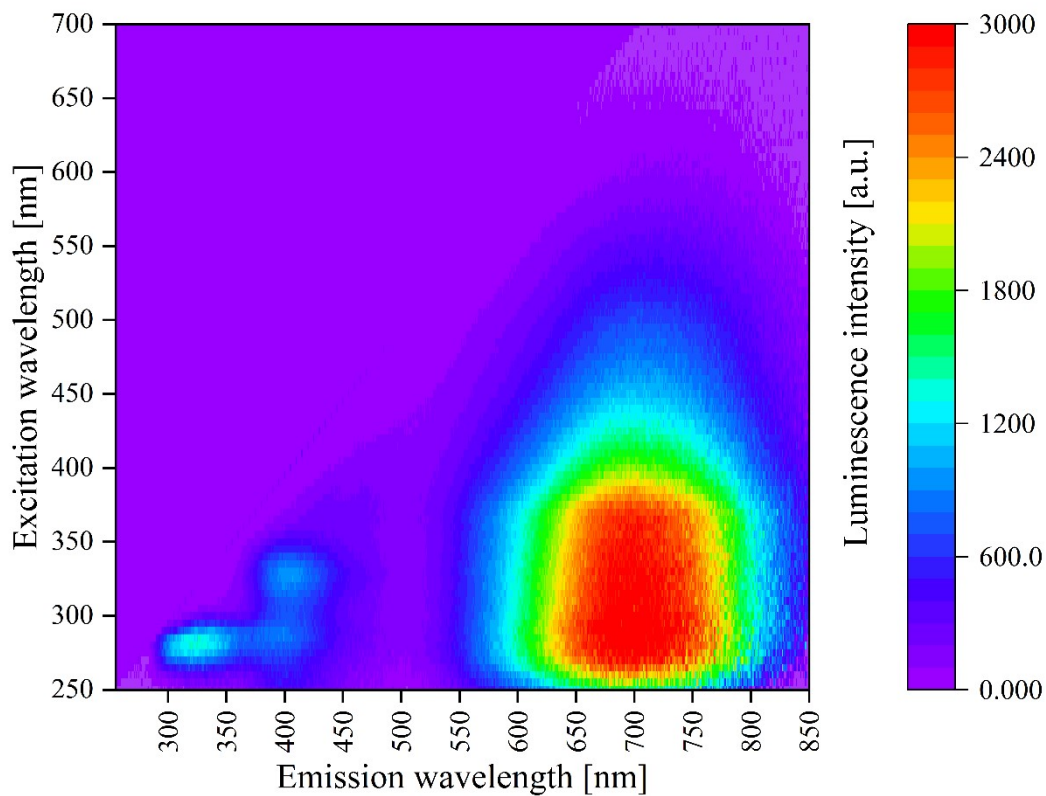


**Figure SI-3:** Excitation-emission luminescence 3D map. Luminescence emission maximum of LGSN-SPION nanocomposite is positioned at around 700 nm ( $\pm 30$  nm) when using the excitation wavelength in the range from 250 to 550 nm. Obviously, the higher the excitation wavelength is, the less energy in it, therefore, the less intensive emission recorded.

## 5. Quantum yield determined for LGSN-SPION via SPION-free sample

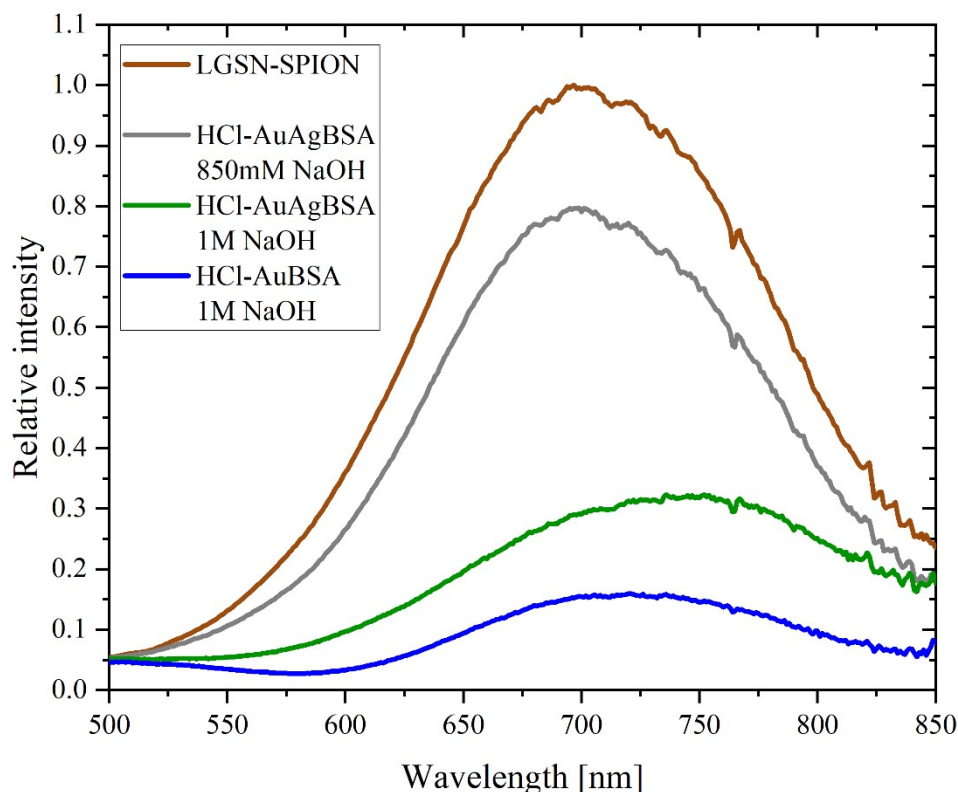


**Figure SI-4:** Relative fluorescence spectra of LGSN-SPION compared with HCl-AuAgBSA and HCl-AuBSA that were prepared as SPION-free samples for fluorescence quantum yield determination. Obviously, the highest similarity with LGSN-SPION is obtained for HCl-AuAgBSA-850mM-NaOH because it manifested itself by the same position of emission maximum as that observed for LGSN-SPION.

**Table SI-6:** Fluorescence quantum yield (FQY) of HCl-AuAgBSA and HCl-AuBSA samples are listed. DCM was used as a standard.

Sample	FQY [%]
HCl-AuAgBSA-850mM-NaOH	5.9
HCl-AuAgBSA (1M NaOH)	2.0
HCl-AuBSA (1M NaOH)	1.2

Evidently, the fine pH adjustment is very crucial not only for the position of emission maximum (Figure SI-3), but also for the FQY value (Table SI-6).

## 6. Photostability of LGSN-SPION in media

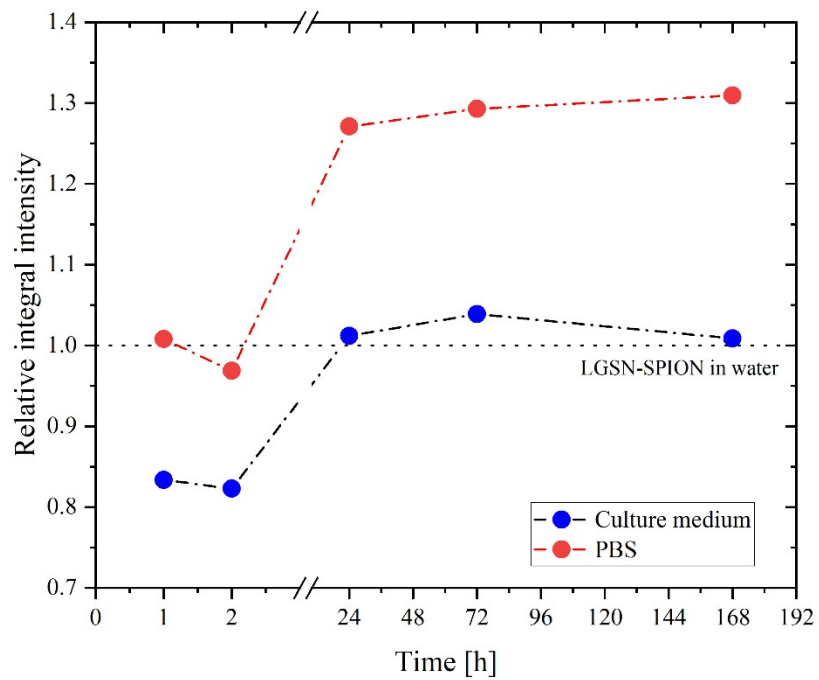


**Figure SI-5:** Relative integral intensity of LGSN-SPION in culture medium and PBS at 37 °C as a function of time. Dot line represents integral fluorescence intensity of LGSN-SPION in water (it was set equal to 1).

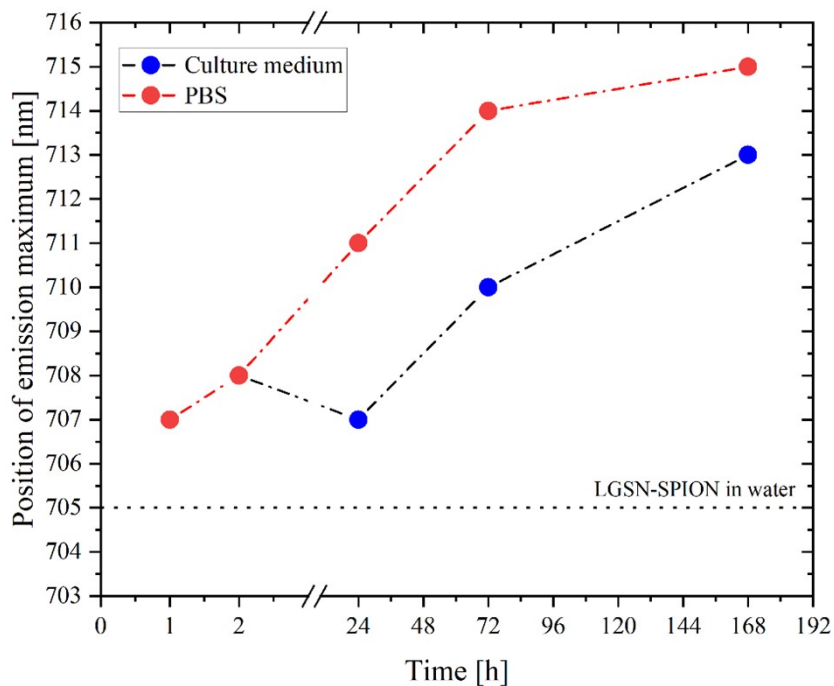


**Figure SI-6:** Emission maximum position of LGSN-SPION in culture medium and PBS at 37 °C observed over time. Dot line represents maximum emission position of LGSN-SPION in water.

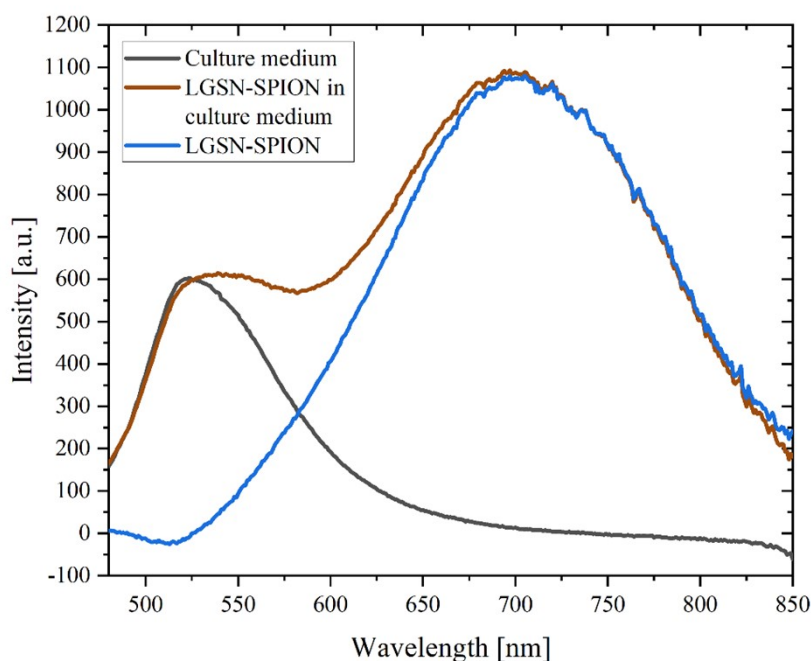


**Figure SI-7:** Fluorescence measurement of culture medium (black line) and LGSN-SPION in culture medium (brown line). The blue spectrum denoted as LGSN-SPION is obtained as a differential spectrum when the signal of culture medium (black line) is subtracted from the experimentally measured LGSN-SPION signal (brown line).

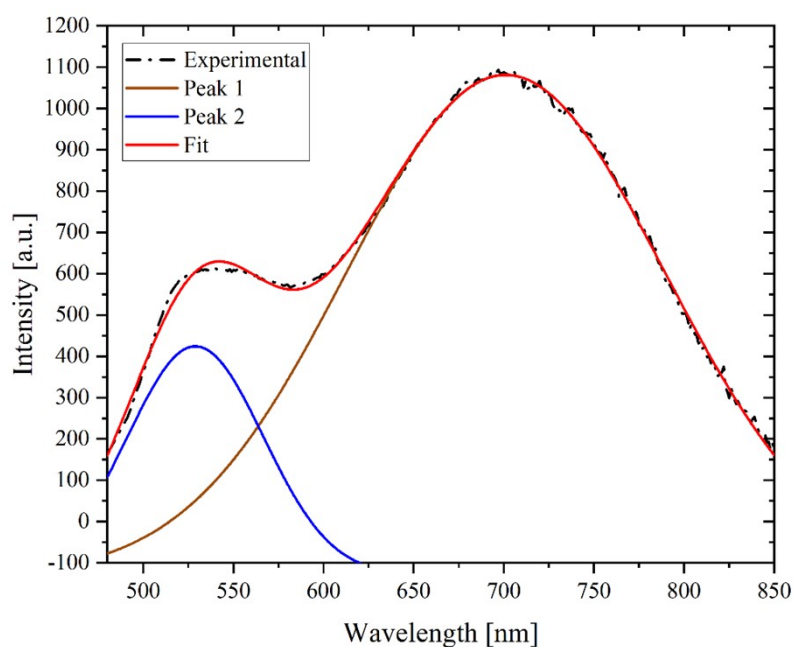


**Figure SI-8:** Red curve is the fit of a representative fluorescence spectrum of LGSN-SPION in the culture medium when deconvolution into two peaks employed: peak 1 (brown line) corresponds to the signal of LGSN-SPION and peak 2 (blue line) is stemming from the culture medium. Dash dot line is the experimentally measured spectrum.

## 7. Cell viability evaluated for LGSN-SPION

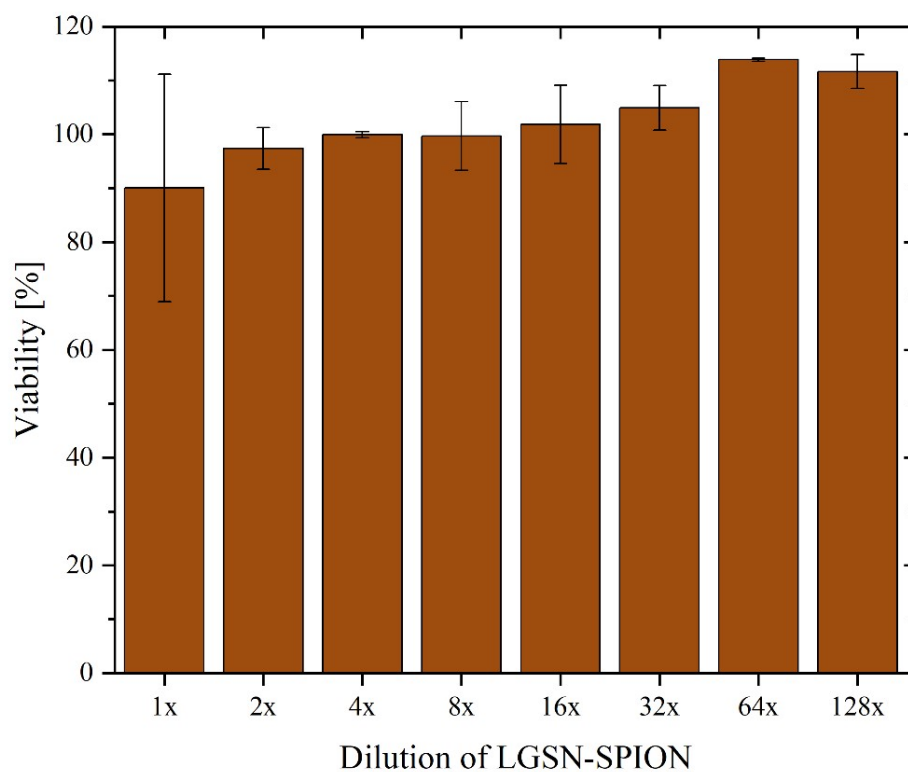


**Figure SI-9:** Graph shows cell viability of LGSN-SPION (including error bars) depending on the sample dilution (i.e., dilution factor is always 2). Dilution 1x means the highest final concentration of LGSN-SPION nanocomposite containing: 0.12 mg/mL Ag, 0.75 mg/mL Au, 0.24 mg/mL Fe, and approx.15 mg/mL albumin.

## 8. *In vitro* optical imaging using LGSN-SPION

**Table SI-7:** Values of fluorescence emission (at 730 nm) of LGSN-SPION nanocomposite in four different concentrations of a representative triplicate recorded in phantoms, excitation 430 nm.

<b>Sample</b>	<b>TM 1</b>	<b>TM 2</b>	<b>TM 3</b>
	Total Emission Photons/s [·10 <sup>9</sup> a.u.]	Total Emission Photons/s [·10 <sup>9</sup> a.u.]	Total Emission Photons/s [·10 <sup>9</sup> a.u.]
<b>100%</b>	6.27	6.90	6.42
<b>75%</b>	7.12	7.01	6.57
<b>50%</b>	6.42	6.26	6.29
<b>25%</b>	4.57	4.64	4.64

Note: TM 1, TM 2, TM 3 are particular samples within a representative triplicate.

9. *In vivo* optical imaging using LGSN-SPION (ex. 500 nm / em. 670 nm)

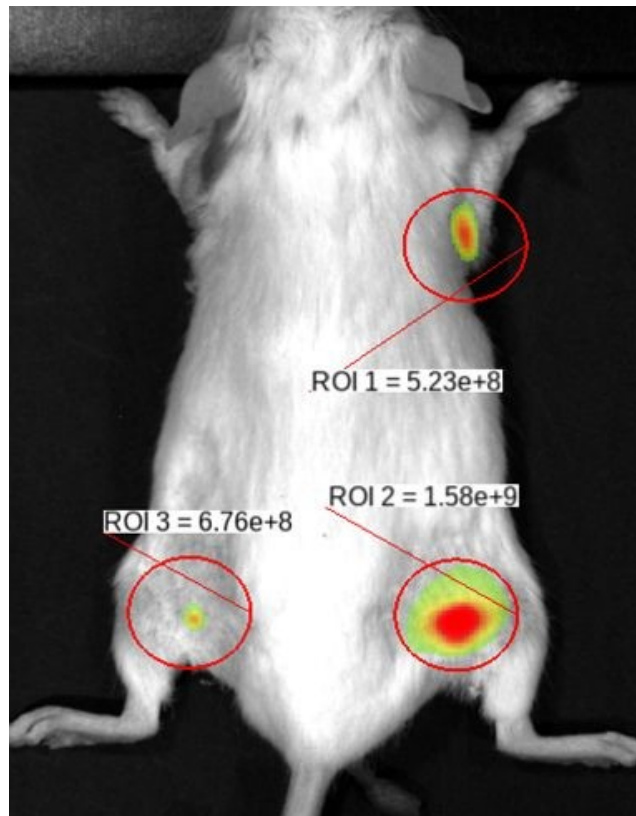


**Figure SI-10:** Optical imaging exploiting LGSN-SPION nanocomposites in a living mouse: excitation at 500 nm and emission at 670 nm.

## 10. Results of relaxometry measurements of LGSN-SPION

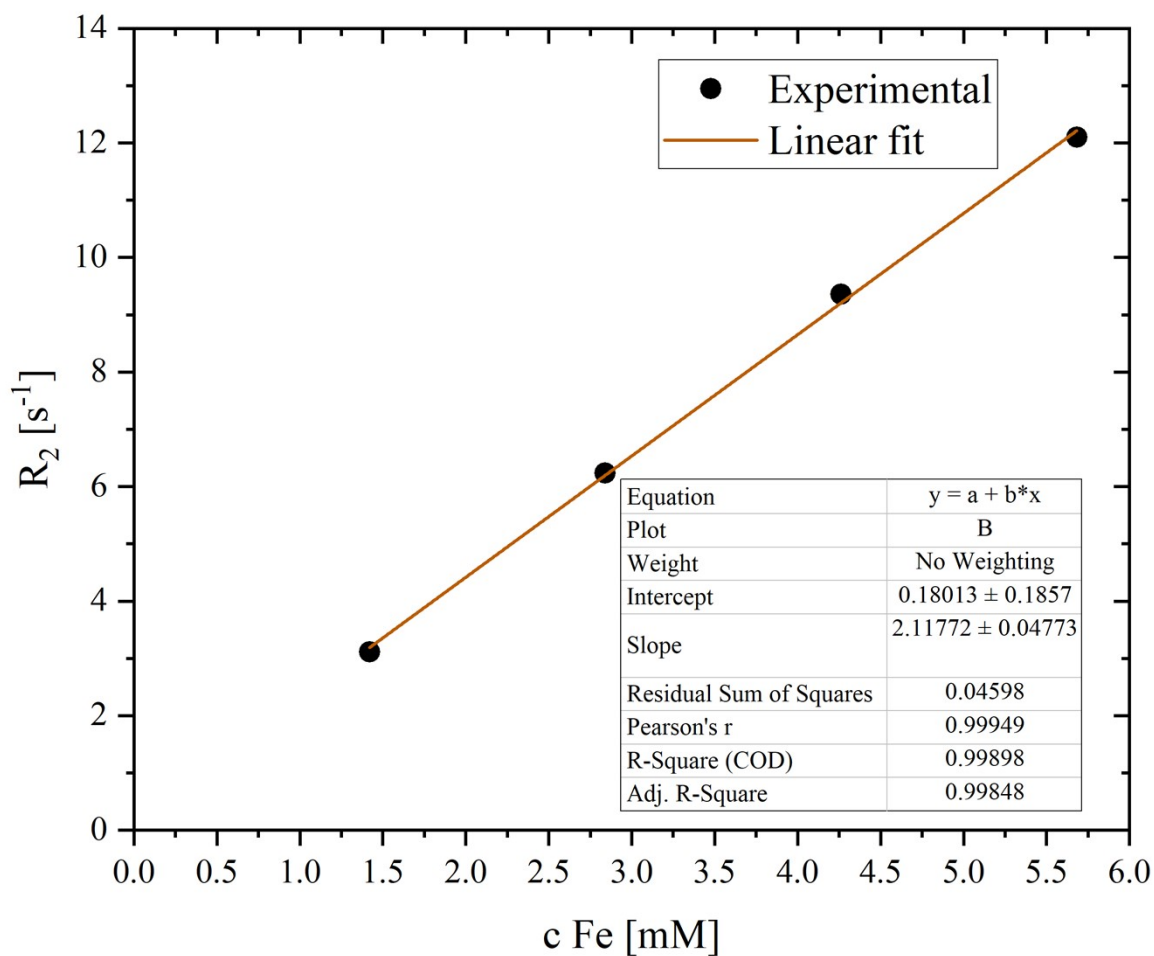


**Figure SI-11:** Relaxation rate  $R_2$  is plotted as a function of iron concentration (determined experimentally by ICP-MS). The slope of the linear fit provides  $r_2$  value, which is calculated for a representative triplicate of LGSN-SPION nanocomposite.

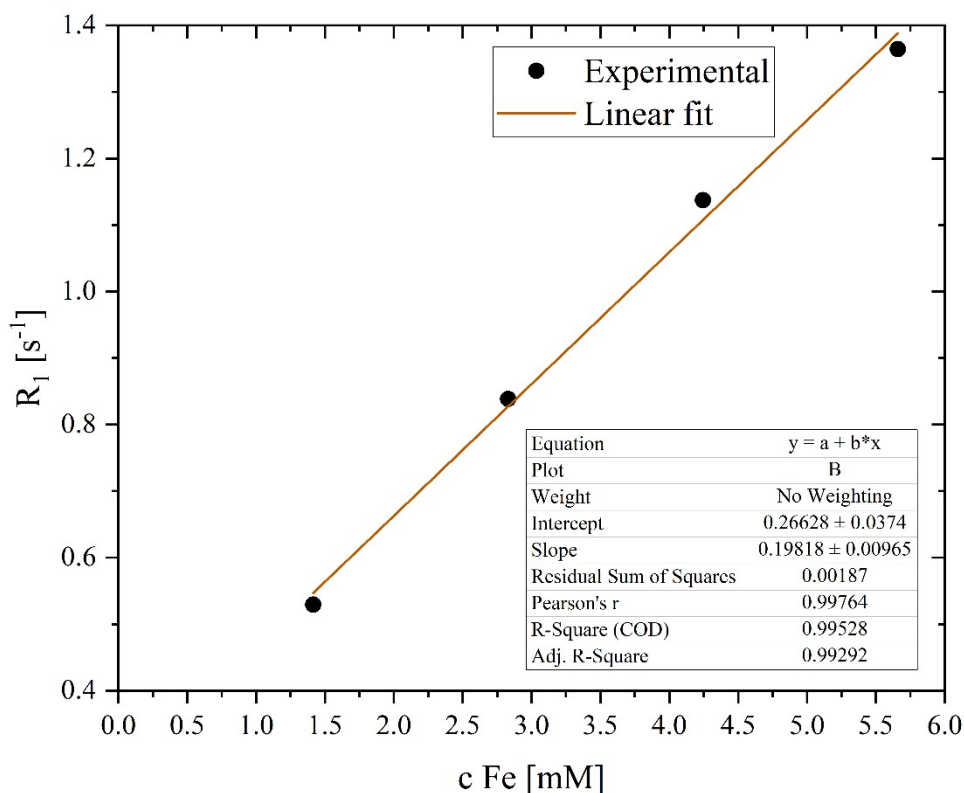


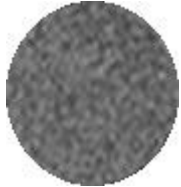
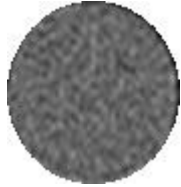
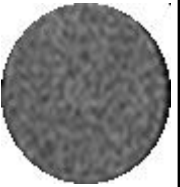
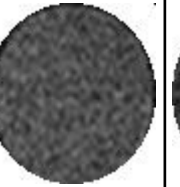
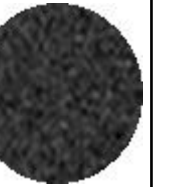
**Figure SI-12:** Relaxation rate  $R_1$  is plotted as a function of iron concentration (determined experimentally by ICP-MS). The slope of the linear fit provides  $r_1$  value, which is calculated for a representative triplicate of LGSN-SPION nanocomposite.

**Table SI-8:** Results of relaxivity measurements performed for a representative triplicate of LGSN-SPION nanocomposite: experimentally determined  $T_1$ ,  $T_2$ ; calculated  $R_1$ ,  $R_2$ ; and averaged  $r_1$ ,  $r_2$  are listed.

	Concentration [mmol/L]	$T_1$ [ms]	$R_1$ [1/ms]	$r_1$ [L·mmol <sup>-1</sup> ·s <sup>-1</sup> ]	$T_2$ [ms]	$R_2$ [1/ms]	$r_2$ [L·mmol <sup>-1</sup> ·s <sup>-1</sup> ]
TM 1,2,3	100%	732.89	1.36	$0.20 \pm 0.01$	83.03	12.04	$2.12 \pm 0.05$
	75%	879.33	1.14		106.88	9.36	
	50%	1192.67	0.84		160.54	6.23	
	25%	1889.33	0.53		321.92	3.11	

## 11. T<sub>1</sub>-weighted MR images of phantoms

**Table SI-9:** T<sub>1</sub>-weighted MR images of phantoms acquired for four different concentrations of a representative LGSN-SPIO sample; corresponding signal-to-noise-ratio (SNR) and contrast-to-noise-ratio (CNR) are listed.

<b>TM 1</b>		<b>100 %</b>	<b>75 %</b>	<b>50 %</b>	<b>25 %</b>	<b>H<sub>2</sub>O</b>
<b>T<sub>1</sub>-weighted</b>						
	<b>SNR</b>	7.43	7.08	6.98	5.49	3.55
	<b>CNR</b>	3.87	3.53	3.43	1.94	-